

Clearance Detection, Evaluation and Reporting System (CDERS)

FINAL REPORT

May 2003

Submitted by

Farhad Bassali
Research Associate
New Jersey Institute of Technology
Electrical and Computer Engineering Department

Dr. Edip Niver
Associate Professor
New Jersey Institute of Technology
Electrical and Computer Engineering Department

Dr. Alain L. Kornhauser
Professor
Princeton University
Department of Operations Research and Financial Engineering



NJDOT Research Project Manager
Edward S. Kondrath

In cooperation with

New Jersey
Department of Transportation
Division of Research and Technology
and
U.S. Department of Transportation
Federal Highway Administration

DISCLAIMER STATEMENT

The contents of this report reflects the views of the author(s) who is (are) responsible for the facts and the accuracy of the data presented herein. The contents do not necessarily reflect the official views or policies of the New Jersey Department of Transportation or the Federal Highway Administration. This report does not constitute a standard, specification, or regulation.

1. Report No. FHWA-NJ-2001-026	2. Government Accession No.	3. Recipient's Catalog No.	
4. Title and Subtitle Clearance Detection, Evaluation and Reporting System (CDERS)		5. Report Date May 31, 2003	
		6. Performing Organization Code NJIT	
7. Author/s Farhad Bassali, Edip Niver and Alain L. Kornhauser		8. Performing Organization Report No.	
9. Performing Organization Name and Address Electrical and Computer Engineering/NJ TIDE Center New Jersey Institute of Technology University Heights Newark, NJ 07102-1982		10. Work Unit No.	
		11. Contract or Grant No. 995916	
12. Sponsoring Organization Name and Address New Jersey Department of Transportation		13. Type of Report and Period Covered 09/01/00-08/31/01	
		14. Sponsoring Agency Code	
15. Supplementary Notes			
16. Abstract The Clearance Detection, Evaluation and Reporting System (CDERS) concept has been developed based on microwave technology at the New Jersey Institute of Technology and vision based system at Princeton University. This is accomplished by utilizing a wide band (500 MHz) signal operating at the 23 GHz band. The validity of the concept was established by building a prototype using waveguide components. Sampling circuits were used to handle the time domain signal processing and display hardware. The prototype demonstrated that sub-centimeter resolution was achieved when measuring the lateral clearances. Future developmental work will address the merits of the proposed concept. This work will reduce the size by utilizing MMIC (Microwave Monolithic Integrated Circuits) technology. It will make use of electronically steerable microstrip patch antennas, appropriate signal processors and improved software design. Lower costs and space efficient units will result. Vision Based Clearance Detection System development has been discussed in the Appendix.			
17. Key Words Time Domain Radar, Clearance Detection, Collision Avoidance			18. Distribution Statement
19. Security Classification (of this report) Unclassified	20. Security Classification (of this page) Unclassified	21. No. Of Pages 30	22. Price Free

Acknowledgments

The authors would like to acknowledge the support provided by the New Jersey Department of Transportation, and the U.S. Department of Transportation Federal Highway Administration and the kind interest and support of the following individuals at the Division of Research and Technology at NJDOT: Mr. William Hoffman, Mr. Nicholas Vitillo and especially to the project manager, Mr. Edward S. Kondrath. Further interest and support from Mr. Jim Perel and Mr. Thomas Fuca of NJDOT are acknowledged. Special thanks are also to Professors Louis Pignataro, David Bernstein and Kyriacos Mouskos for their support and encouragement at the NJ TIDE Center at NJIT/Princeton University.

TABLE OF CONTENTS

	<u>Page</u>
SUMMARY	1
INTRODUCTION	1
Objective	1
Important Features of the Proposed System	2
Potential Benefits of the Project	2
Technology Outlook	2
PROTOTYPE DEVELOPMENT	4
Theory of Operation	4
Feasibility Range	6
Construction and Packaging	7
Installation Scheme	7
Anticipated Cost	8
Interference Avoidance	9
TEST RESULTS	9
Antenna Feasibility	10
VISION BASED CLEARANCE DETECTION SYSTEM	16
CONCLUSIONS	16
REFERENCES	18
APPENDIX-Autonomous Vehicle Vision Guidance with Difference Image and Optical Flow	19

LIST OF FIGURES

	<u>Page</u>
Figure 1. Block diagram of the developed prototype system.	4
Figure 2. Layers of the time domain radar.	7
Figure 3. Typical Installation.	8
Figure 4. Field tests were performed using a radar, constructed with waveguide components installed on the front bumper of the vehicle.	9
Figure 5. 64-Element planar array.	10
Figure 6. 8-Way power splitter.	10
Figure 7. Aperture-coupled element.	11
Figure 8. Far field radiation patterns of 8-element patch antenna arrays.	12
Figure 9. Radiation pattern of a linear array, 8-elements, 0.65λ spacing, 4-bit	12
Figure 10. E-plane radiation pattern of a planar 64-element array.	13
Figure 11. H-plane radiation pattern of a planar 64-element array.	13
Figure 12. Planar array, Taylor amplitude distribution, 0.65λ spacing.	14
Figure 13. 3-Dimensional radiation pattern of a 64-element uniform array.	15
Figure 14. 3-Dimensional radiation pattern of a 64-element Taylor array.	15
Figure 15. Phase Shifter Unit Cell Using 3-dB Coupler.	16
Figure 16. Dividing image areas.	21
Figure 17. Determining optical flow.	23
Figure 18. Optical flow field when approaching the leading vehicle.	25
Figure 19. Optical flow field when approaching the lane mark.	25
Figure 20. The Simulator.	27

LIST OF TABLES

	<u>Page</u>
Table 1. Components of the Current System and Goals.....	5

SUMMARY

The Clearance Detection, Evaluation and Reporting System (CDERS) has been developed based on microwave and vision technologies. These new concepts for a high resolution collision avoidance warning device for vehicles, were developed by the New Jersey Institute of Technology and Princeton University. One of the concepts utilizes a wide band (500 MHz) microwave signal operating at the 23 GHz band. The validity of the concept was established by building a prototype using waveguide components. Sampling circuits were used to handle the time domain signal processing and the display hardware. The prototype demonstrated that sub-centimeter resolution was achieved in measuring the lateral clearances. Future developmental work will address the merits of the proposed concept. This work will reduce the size by utilizing MMIC (Microwave Monolithic Integrated Circuits) technology. It will make use of electronically steerable microstrip patch antennas, appropriate signal processor and improved software design. Lower costs and space efficient units will result. Vision Based Clearance Detection System development has been discussed in the Appendix.

INTRODUCTION

Objective

The objective of this project was to develop clearance detection for vehicles while in motion. A major goal of this project was to design an inexpensive clearance monitoring device. This device was to alert the driver of the presence of vehicles in the vicinity of his/her vehicle. The potential system using steerable narrow beam microstrip patch antennas will be installed on the four sides of a vehicle. The system would then provide an accurate display of the objects in the surrounding vicinity (360 degrees) and thereby could alert the driver to take measures against potential collisions. This report discusses the merits of these concepts, the work progress, feasibility of a low cost space efficient unit and enumerates the future work schedule.

Important Features of the Proposed System

The major features of the proposed and partially developed system are:

- Installed on four sides of vehicle (only front section has been built and tested)
- Provides accurate distance measurements to the operator of the vehicle by using a wide band time domain signal
- Alerts the operator of a potential collision based on a selected threshold clearance
- Narrow beam antenna with beam steering provides wide angle coverage and avoids returns from multiple vehicles
- Microstrip antennas are placed conformally on the vehicle body surfaces
- Appropriate coding allows simultaneous operation of different vehicles without interference (future development)
- State-of-the-art MMIC allows inexpensive and space efficient implementation
- Electronic beam steering allows fast and reliable operation.

Future developmental work has to be performed in order to reduce the size by utilizing MMIC (Microwave Monolithic Integrated Circuits) technology and electronically steerable microstrip patch antennas. In addition, appropriate signal processor and software design should be performed.

Potential Benefits of the Project

The vehicular collision avoidance device, assists drivers in avoiding accidents by alerting via audio signals and visual displays. Accidents due to poor visibility could potentially be avoided by utilizing the proposed device.

Technology Outlook

The development of automotive sensing technology began in the 1970's and until the 1980's they were operating at millimeter-wave or microwave bands. Due to

the complexity and high cost of microwave and millimeter-wave devices, optical pulse radars with infrared laser diodes were first developed as potential automotive sensors. However, safety standards concerning eyesight protection restrict the output power of optical radars with laser diodes. Rain, fog, and snow reduce the range of optical devices when they are most needed [1].

Due to the advent of MMIC technology, the K-band range devices are the most promising. Fast signal processors and major advancements in Ultra Wide Band (UWB) technology [2], allows the time domain system to achieve higher spatial resolution. Special coding schemes and small duty cycles of UWB time domain systems may be utilized to avoid interference between motorists operating similar systems in close vicinity.

An important concern is the ability to cover the area around a vehicle using narrow beams to distinguish between various objects. The technology for electronically steerable beam antennas is achievable for this application. Thus a time domain radar in K-Band (18-26.5 GHz) with a practical antenna size and based on inexpensive MMIC devices appears to be the most appropriate choice. Utilization of K-Band microwave region provides insignificant attenuation due to heavy rain (16 mm/hr) 0.2 dB for a 30 meters range [3] and negligible attenuation less than 0.05 dB due to heavy fog or cloud (2.3 gm/m^3).

Previous work done in this field used more expensive hardware with less performance than the proposed concept, e.g., the FM-CW scheme is prone to interference in the presence of other vehicles in the close vicinity [1]. Multiple horn antennas were used to resolve different directions for different targets [4]. The usage of lens antennas [5] on a flat surface on the vehicle makes such an approach impractical due to excessive volume they occupy.

PROTOTYPE DEVELOPMENT

A prototype was built using waveguide components (See Table1). Field tests were performed and a range of 20 meters was achieved. Detailed explanation of the developed prototype is given below.

Theory of Operation

Figure1 depicts the system block diagram. A wide bandwidth of 500 MHz is selected in order to obtain a high resolution. Table 1 lists the components of the current system and the desired system based on MMIC technology.

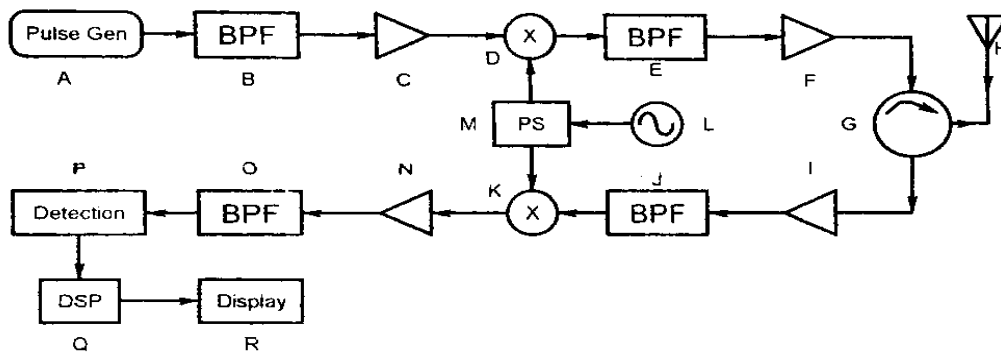


Figure 1. Block diagram of the developed prototype system.

The transmitter is composed of a Fast Rise Time Pulse Generator (A) followed by a Band Pass Filter (B) centered at 1.75 GHz. As the pulse is applied to the

filter, a 1.75 GHz burst with a bandwidth of 500 MHz is generated which is amplified by amplifier (C) and up-converted by the Frequency Mixer (D). The Oscillator (L) signal is divided by the power splitter and supplied as the Local Oscillator for the Frequency Mixers (D) and (K). The Band Pass Filter (E) allows

Table 1. Components of the Current System and Goals.

SECTION	DESCRIPTION	CURRENT SYSTEM	GOALS
A	Fast Rise Time Step/Impulse Generator	HP1105B	Step Recovery Diode
B	1.5-2.0 GHz Band Pass Filter	Edge Coupled Micro-Strip Line	Comb-Line, Strip- Line
C	1.5-2.0 GHz Amplifier	Mini-Circuits	MMIC
D	Frequency Mixer	Ortho-Mode, Wave-Guide Mixer	Gilbert Cell MMIC
E	23.0-23.6 GHz Band Pass Filter	Wave Guide Cavity	Edge Coupled Strip Line
F	23.0-23.6 GHz Amplifier	Microwave dB	MMIC
G	23.0-23.6 GHz Circulator	Wave Guide Ports	Micro Strip Line
H	Antenna	Pyramidal Horn (Linear Polarization) 8.4 x 10.2 x 24 cm	Steerable Micro-Strip Patch Antenna (Circular Polarization) 12 x 15 x 0.2 cm
I	23.0-23.6 GHz Low Noise Amplifier	Microwave dB	MMIC, 1.5 dB NF
J	23.0-23.6 GHz Band Pass Filter	Wave-Guide Cavity	Edge Coupled Strip Line
K	Frequency Mixer	Ortho-mode, Wave-Guide Mixer	Gilbert Cell MMIC
L	Local Oscillator	Gunn Diode Oscillator (GDO)	MMIC Dielectric Resonator Oscillator(DRO)
M	Power Divider	Wave-Guide	MMIC
N	1.5-2.0 GHz Amplifier	Mini-Circuits	MMIC
O	Detection Circuit	HP 1815B/1817A	Custom High Speed Sampling Circuit
	Overall Size		13 x 16 x 0.6 cm
	Cost		< \$ 40

only the upper side band to be supplied to the Microwave Amplifier (F). The burst is routed through the circulator (G) and transmitted to the space by the

Antenna (H). The returned bursts from the targets are received by the Antenna (H) and routed to the receiver via the circulator (G). The bursts are amplified by the Low Noise Amplifier (I). The Band Pass Filter (J) passes the bursts and suppresses the noise at the image frequency band. The Frequency Mixer (K) down-converts the burst to 1.75 GHz. The signal is amplified by the Amplifier (N). The Band Pass Filter (O) suppresses the out of band noise. Due to wide bandwidth of the signal, a sampling detection scheme is used via Detector (P). The Digital Signal Processor (Q) is used to estimate the distance of the surrounding targets. The relative locations of targets are displayed on a Graphical Display (R). Audio alerting signals could aid the operator of the vehicle of possible collisions.

Feasibility Range

Based on the available components that were procured for the project, the range of the radar is calculated to be 76 meters given by:

$$R_{\max} = \left(\frac{P_t G^2 \lambda^2 \sigma}{(4\pi)^3 k T B F (S/N)_{\min}} \right)^{1/4}$$

DEFINITION OF PARAMETERS

R_{\max} = Range
 P_t = Transmit Power
 G = Antenna Gain
 λ = Wave Length
 σ = Radar Cross Section
 k = Boltzman's Constant
 T = Temperature °Kelvin
 B = Bandwidth
 F = Noise Factor
 $(S/N)_{\min}$ = Minimum Signal to Noise Ratio

SELECTED PARAMETER

$P_t = 17 \text{ dBm} = 0.051 \text{ W}$
 $G = 289 \text{ W/W}$
 $\lambda = 0.0129 \text{ m}$
 $\sigma = 0.6 \text{ m}^2$
 $k = 1.38 \times 10^{-23}$
 $T = 300 \text{ °K}$
 $B = 500 \text{ MHz}$
 $F = 2$
 $(S/N)_{\min} = 3$
 $R_{\max} = 76 \text{ m}$

Construction and Packaging

Figure 2 depicts the proposed construction of the radar in four different layers. The antenna is composed of two layers of dielectric materials: the Feed Layer and the Patch Layer. The external radome layer protects the patch layer of the antenna. The circuit layer contains the MMIC's and the Phase shifters for antenna steering. For an antenna gain of 300 at 23 GHz, the patch antenna will occupy an area of 65 cm^2 ($8.1 \text{ cm} \times 8.1 \text{ cm}$). This gain corresponds to a beam width of 10 degrees.

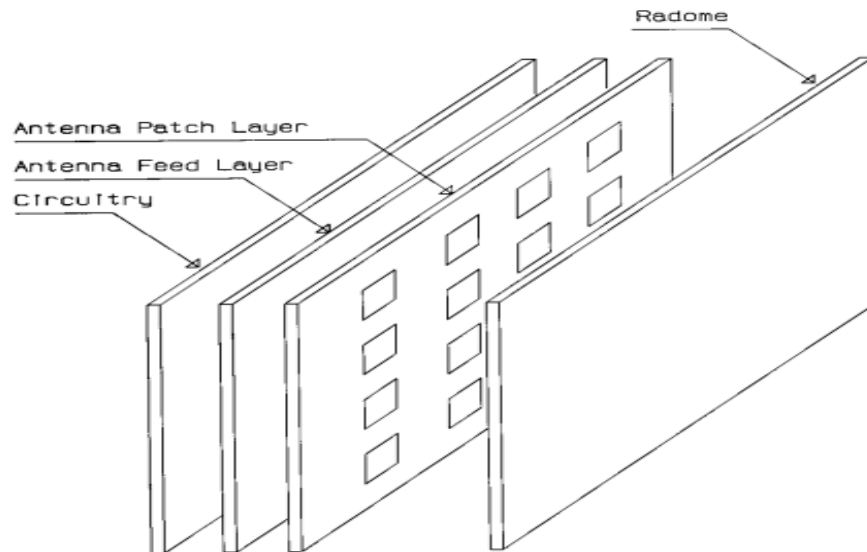


Figure 2. Layers of the time domain radar.

Installation Scheme

Figure 3 depicts installation of the radar on a vehicle. In order to have full coverage of the surroundings of the vehicle, four radars are to be used, one on

each side of the vehicle. Each side unit of the radar is equipped with electronically steerable flat antennas. Steering of the antenna beams enables it to scan the entire surroundings of the vehicle. Since an antenna with a relatively narrow beam is selected (10 degrees), returns from multiple targets could be distinguished by software.

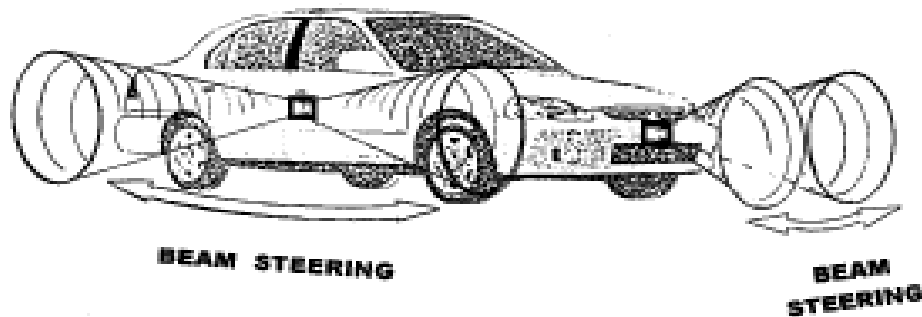


Figure 3. Typical Installation.

Anticipated Cost

K-band microwave transceivers with advances in semiconductor technology, are typically manufactured at a cost of only several dollars. The cost for a custom sampling circuit is estimated to be around \$10. For an 8.1 cm X 8.1 cm patch antenna which meets the requirements, the cost could be brought to under \$ 4 in large quantities. Other components such as various filters and Digital Signal Processors (DSP's) and the packaging is estimated to be about \$10. The cost of assembly and testing is estimated to be under \$5. Hence, the total manufacturing cost could be less than \$30.

Interference Avoidance

A low duty cycle burst in a coded envelope allows many users to operate within the chosen band. This feature will permit simultaneous use of similar systems in vehicles all within the same vicinity, resulting in a very small probability of crossed messages.

TEST RESULTS

Field tests were performed. Figure 4 is a photograph of the installed proto-typed system constructed from waveguide components. The preliminary tests indicated the following:

- The radar responded well to vehicles, human targets and buildings. This confirms the appropriate choice for the selected frequency band for avoiding accidents with humans, objects, other vehicles and buildings.
- A range of 15-20 meters was obtained for cars, measured in dry weather conditions.



Figure 4. Field tests were performed using a radar, constructed with waveguide components installed on the front bumper of the vehicle.

Antenna Feasibility

The Figure 5 below depicts the scheme of the proposed K-Band Phase array antenna with 64 elements with 0.65λ spacing between the elements for the next phase prototype.

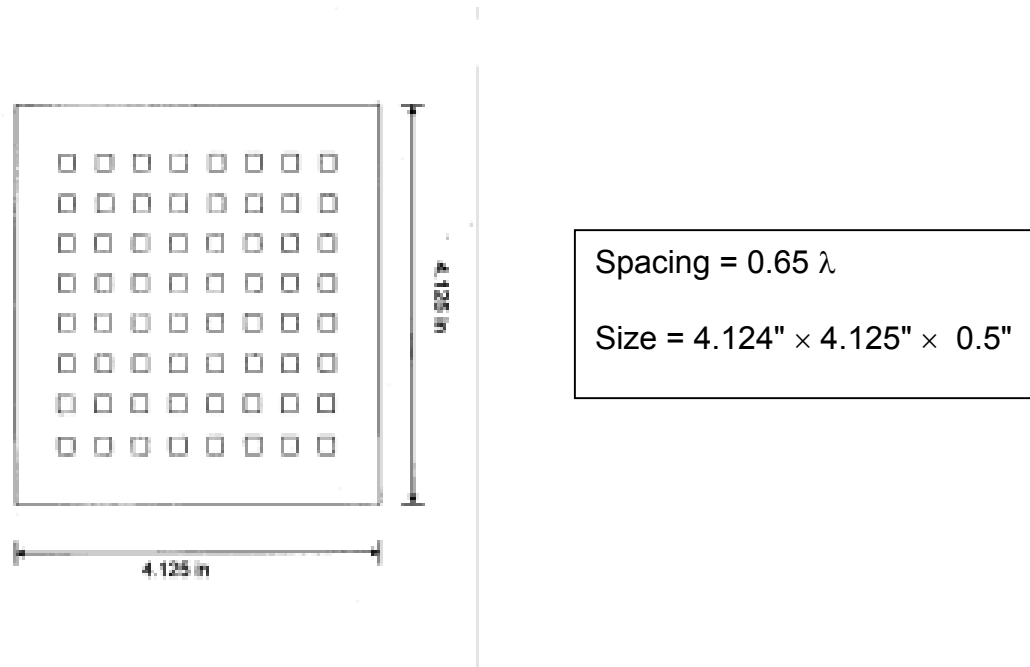


Figure 5. 64-Element planar array.

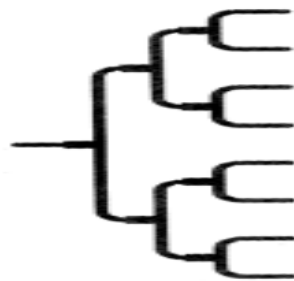
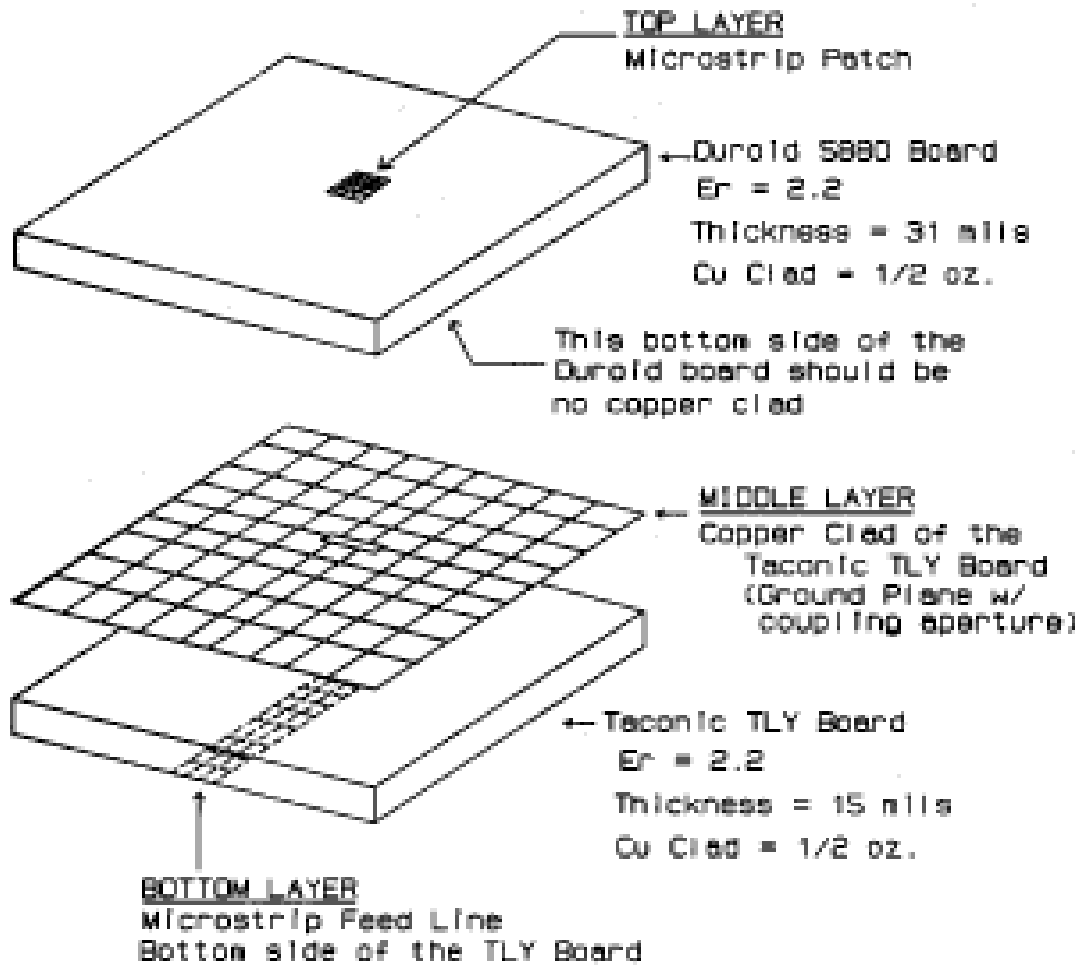


Figure 6. 8-Way power splitter.

This figure depicts the feed network for each column of the array of the proposed antenna.

Figure 7 depicts construction of one element of an aperture-coupled network feed structure.



NOTE:

The grid () means solid copper clad of the board.

Figure 7. Aperture-coupled element.

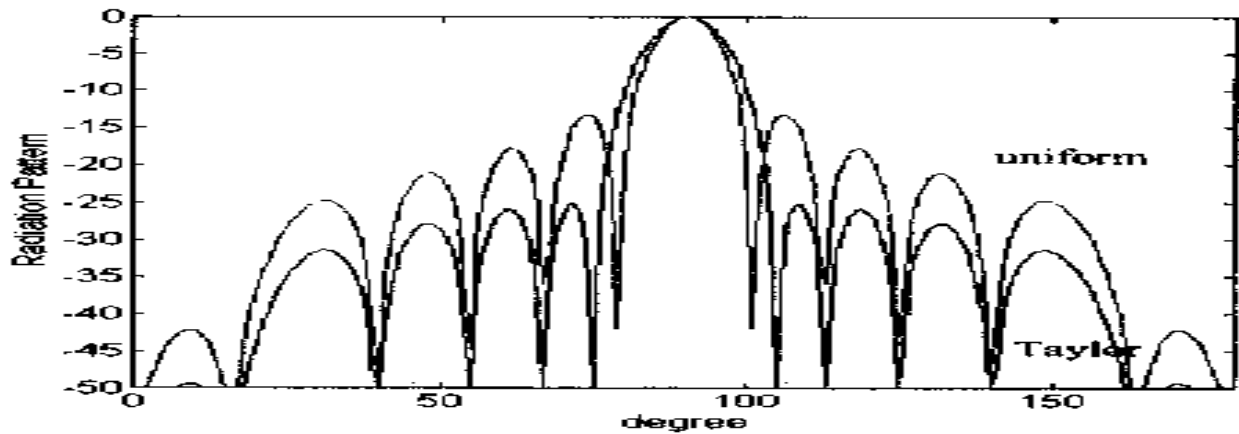


Figure 8. Far field radiation patterns of 8-element patch antenna arrays.

This figure depicts the predicted radiation patterns for the 8-element patch antenna arrays with Taylor and uniform distributions, respectively. The usage of Taylor distribution reduces sidelobes by 12 dB compared to uniform distribution.

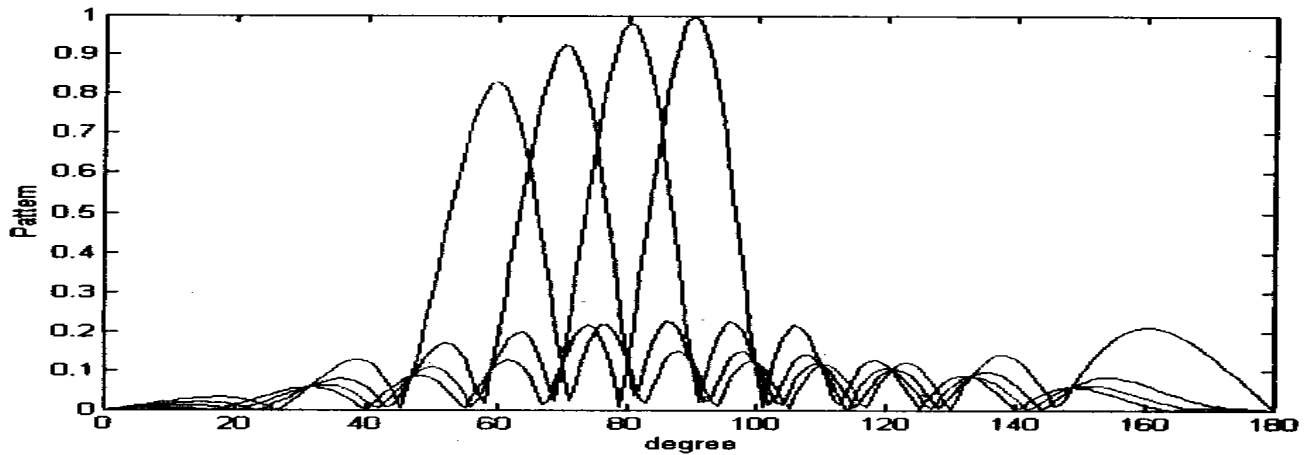


Figure 9. Radiation pattern of a linear array, 8-elements, 0.65λ spacing, 4-bit phase shifter.

Figure 9 depicts 4 major different radiation patterns from possible 16 patterns produced by using a 4-bit phase shifter.

Figures 10 and 11 depict the radiation patterns of 64-element array in E & H planes.

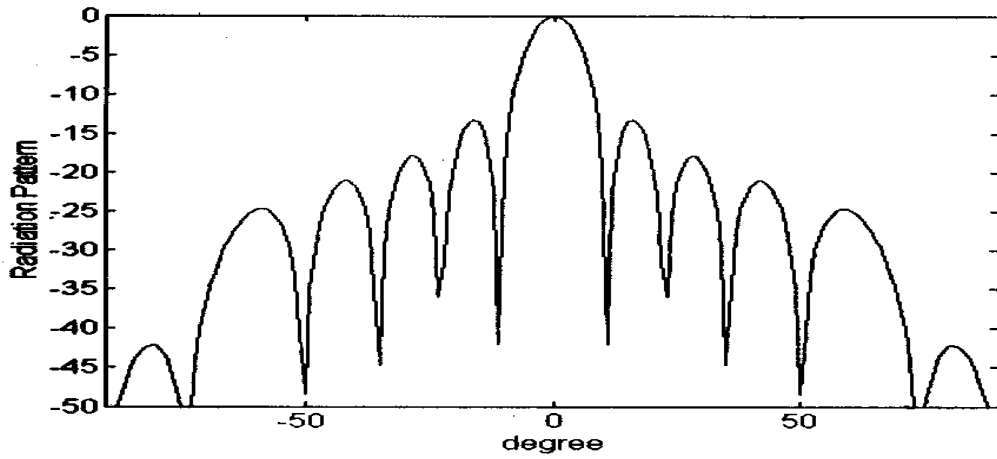


Figure 10. E-plane radiation pattern of a planar 64-element array.

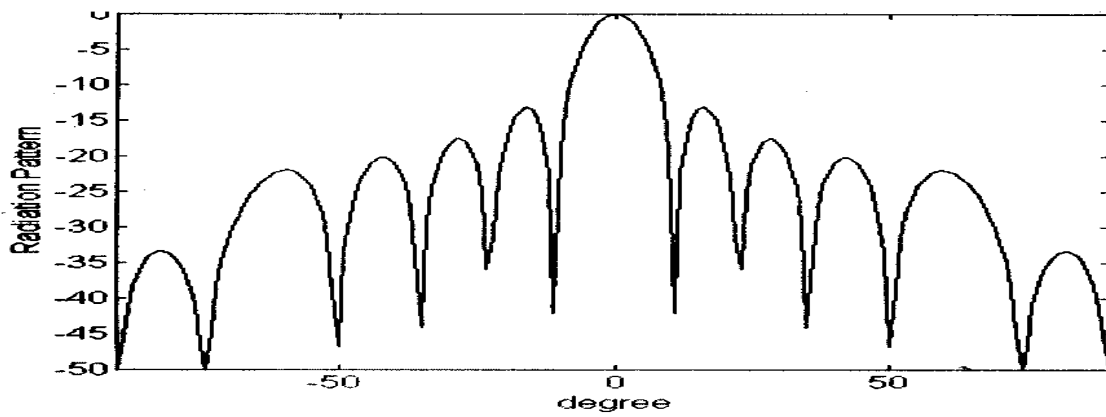


Figure 11. H-plane radiation pattern of a planar 64-element array.

0.154	0.233	0.331	0.393	0.393	0.331	0.233	0.154
0.233	0.350	0.499	0.592	0.592	0.499	0.350	0.233
0.331	0.499	0.711	0.843	0.843	0.711	0.499	0.331
0.393	0.592	0.843	1	1	0.843	0.592	0.393
0.393	0.592	0.843	1	1	0.843	0.592	0.393
0.331	0.499	0.711	0.843	0.843	0.711	0.499	0.331
0.233	0.350	0.499	0.592	0.592	0.499	0.350	0.233
0.154	0.233	0.331	0.393	0.393	0.331	0.233	0.154

Figure 12. Planar array, Taylor amplitude distribution, 0.65λ spacing.

This figure depicts the excitation coefficients for Taylor amplitude distribution in the array.

Figure 13 and Figure 14 depict three dimensional radiation patterns of a uniform and Taylor arrays, respectively.

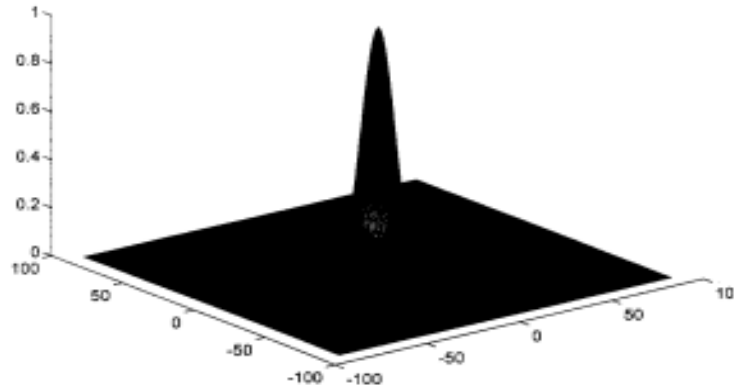


Figure 13. 3-Dimensional radiation pattern of a 64-element uniform array.

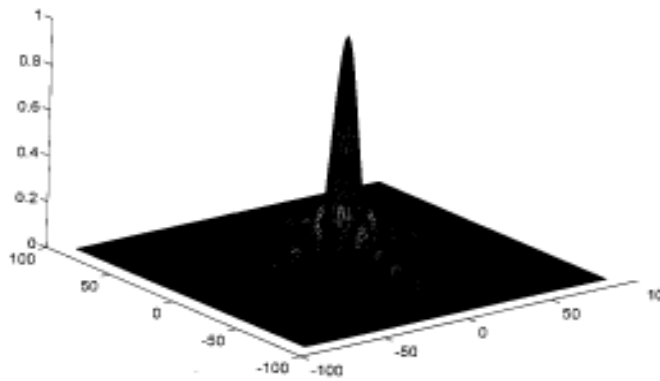


Figure 14 3-Dimensional radiation pattern of a 64-element Taylor array.

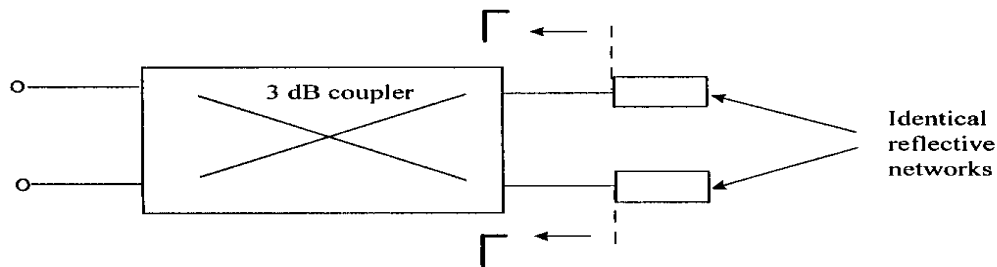


Figure 15. Phase Shifter Unit Cell Using 3-dB Coupler.

This figure depicts typical phase shifter cell configuration to be used in the future.

VISION BASED CLEARANCE DETECTION SYSTEM

As a precursor to the vision-based clearance detection system, the autonomous vehicle vision guidance problem based on the sequential images taken by a camera mounted in the front of the vehicle was studied, by researchers at Princeton University. They employed the difference image and the optical flow field scheme. They proposed a real time computer vision scheme to autonomously navigate the vehicle following the lane and avoiding collision with the leading vehicle. To test the scheme, a simulator was built with OpenGL, a popular graphic language. Results showed that this scheme is reasonable. The detailed results are presented in the Appendix.

CONCLUSIONS

Major milestones of the projects were completed successfully. A prototype was built which achieved the desired performance and confirmed the validity of the proposed concept. Remaining is the development of a flat electronically steerable antenna and implementation of MMIC design for further miniaturization

and cost reduction. The feasibility studies that were performed indicate that using an 8×8 element provides a sufficiently narrow beam width necessary for the intended application. In addition, further work in signal processing and software development is necessary to finalize the concept into a commercially viable product. Vision based clearance detection has proven to be feasible.

REFERENCES

- [1] Robert F. White, Engineering Considerations for Microwave Communications Systems. 1981, GTE Lenkurt Incorporated, San Carlos, California, pp. 48, refer to graphs D & H.
- [2] T. Saito, N. Okubo, Y. Kawasaki, O. Isaji, and H. Suzuki, "An FM-CW Radar Module With Front-End Switching Heterodyne Receiver", *1992 IEEE MTT-S International Microwave Symposium Digest*, Vol. 2 (June 1992), pp.713 - 716.
- [3] Juregen Detlefsen, Thomas Troll, Michael Rozmann, and Willi Zeilinger, "System Aspects and Design of an Automotive Collision Warning PN Code Radar Using Wavefront Reconstruction", *1992 IEEE MTT-S International Microwave Symposium Digest*, Vol. 2 (June 1992), pp.625 - 632.
- [4] H. Roe and G. S. Hobson,. "Improved Discrimination of Microwave Vehicle Profiles", *1992 IEEE MTT-S International Microwave Symposium Digest*, Vol. 2 (June 1992), pp.717 - 724.
- [5] Warren Webb "Ultra wide band: An Electronic Free Lunch?" *December 21, 2000 EDN*, pp. 85-92.

APPENDIX-Autonomous Vehicle Vision Guidance with Difference Image and Optical Flow

Alain L. Kornhauser

Department of Operations Research and Financial Engineering
Princeton University, Princeton, NJ 08544
Email: alaink@princeton.edu
Tel: (609) 258-4657, Fax: (609) 258-1270

Tongqiang Wu

Department of Operations Research and Financial Engineering
Princeton University, Princeton, NJ 08544
Email: twu@princeton.edu
Tel: (609) 258-4411, Fax: (609) 258-4363

Abstract

The autonomous vehicle vision guidance problem based on the sequential images taken by a camera mounted in the front of the vehicle was studied. Employing the difference image and the optical flow, we proposed a real time computer vision scheme to autonomously navigate the vehicle following the lane and avoiding collision with the leading vehicle. To test the scheme, we built a simulator with OpenGL, a popular graphic language. The result showed that this scheme is reasonable. It is a new approach to the autonomous vehicle vision guidance problem.

Key Words: autonomous vehicle, computer vision, difference image, optical flow.

INTRODUCTION

Autonomous vehicle guidance is one of the most challenging areas in the Intelligent Transportation System. There are several famous autonomous guidance systems around the world, such as ALV (Autonomous Land Vehicle) at University of Maryland, NavLab at Carnegie-Mellon University (1) and VITA II (Vision Technology Application) in Germany (2).

Plenty of researchers work on the vehicle guidance problem too. They employed different approaches to the problem. Schiffmann et al. (3) employed the radar sensor to observe the trajectories of leading vehicles for determining the shape of the road. Kornhauser (4) studied the lateral control by neural network approaches. H-infinity controller (5) (6) is another way to deal with the lateral control. Stiller (7) applied the stereo vision technology. Meier et al.'s (8) approach was based on region growing. Betke et al. (9) applied template matching to recognize the cars. Weng et al. (10) used the point correspondences among image sequences to analyze the motion problem. Optical flow is a popular approach for vision guidance (11). It is caused by the relative motion between the environment and the vehicle. We would employ the optical flow in the vision guidance scheme in this paper.

We consider the freeway vehicle navigation problem. The color of the road surface is assumed almost uniform but that of other objects maybe non-uniform. There is no shade of the trees or interchange on the road. The camera is mounted on the middle line of the test vehicle and faced forward. The test vehicle is required to stay on the same lane when going forward. If there is no vehicle or blocking object in front of the test vehicle, it should accelerate to speed limit. If there is vehicle or blocking object in front of the test vehicle, it should decelerate or stop to avoid the collision. If the road has a curvature, the test vehicle should adjust the steering to follow and stay within the lane.

The calculation of difference image and optical flow will be introduced first. Then we propose the vision guidance scheme. The results are reported followed by the discussion and future work. At the end, the conclusion is addressed too.

DIFFERENCE IMAGE AND OPTICAL FLOW FIELD

Dividing Image Areas

For later convenience, we divided the image frame into different parts. Within an image frame, the left and right upper corners are less important. We neglect them and the remaining area is called F . (Note: F may be the whole image frame too.) F consists of F_L and F_R where the middle vertical line divides them (FIGURE 16, (a)). If we use a horizontal line to divide the area F from the middle, we got

F_{TOP} and F_{BOT} (FIGURE 16, (b)). Similarly, the left lower part is called $F_{L,BOT}$ and the right lower part is called $F_{R,BOT}$ (FIGURE 16, (c)). The horizontal dividing lines in FIGURE 16 (b) and (c) are not necessarily the same.

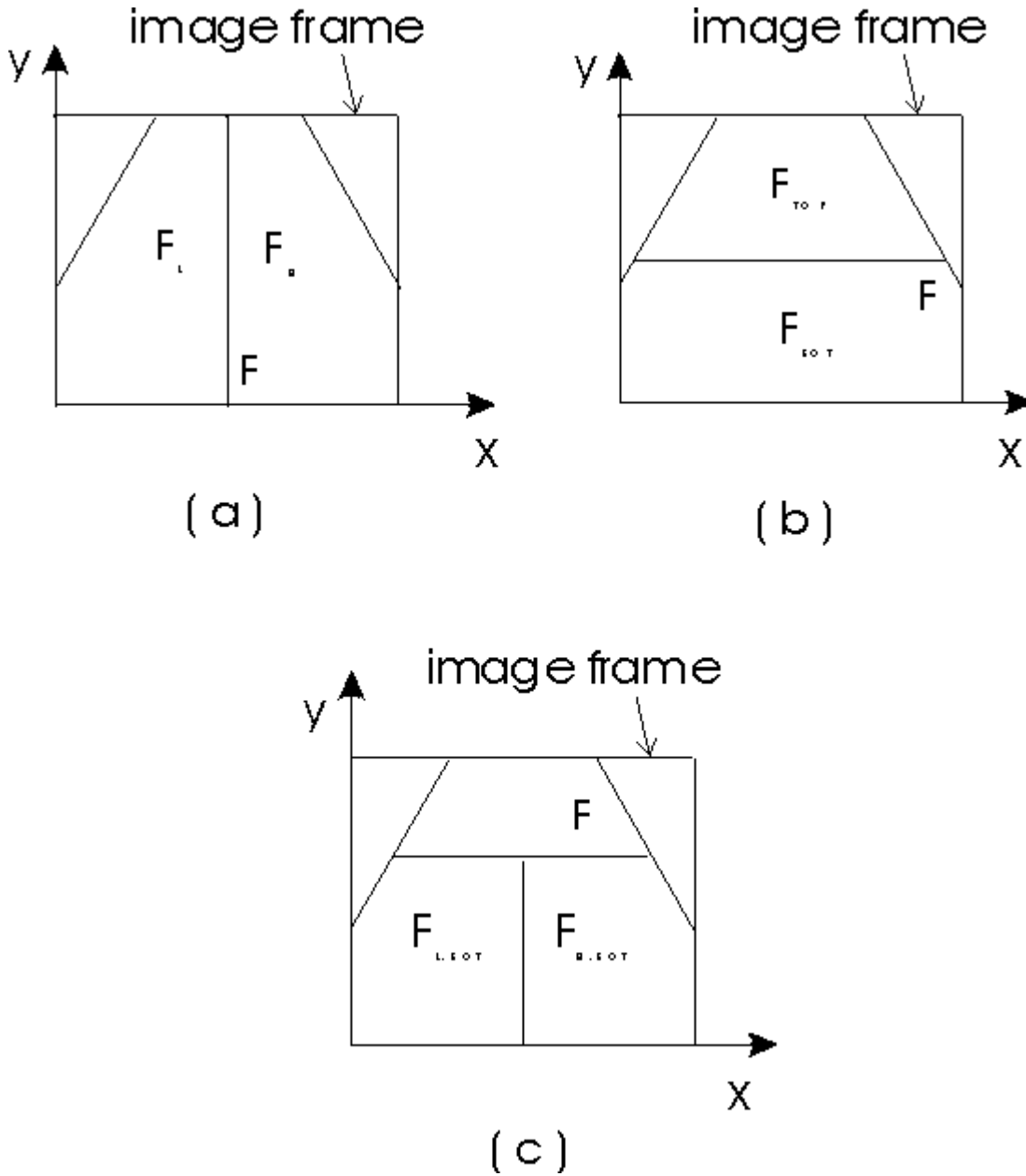


Figure 16. Dividing image areas.

- (a) $F = F_L + F_R$
- (b) $F = F_{TOP} + F_{BOT}$
- (c) $F_{L,BOT}$ and $F_{R,BOT}$

Determining Difference Image

Denote the brightness of point (x,y) at time t as $B(x,y,t)$. Define the difference image $D(x,y,t)$ (12) as:

$$D(x,y,t) = \begin{cases} 1 & \text{if } |B(x,y,t) - B(x,y,t-1)| > T_D \\ 0 & \text{otherwise} \end{cases} \quad (1)$$

where the T_D is a threshold.

The total number of weighted pixels with $D(x,y,t)=1$ in F at time t is

$$D(F,t) = \sum_{(x,y) \in F} W_{D,F}(x,y) D(x,y,t) \quad (2)$$

$$\text{where } W_{D,F}(x,y) \text{ is a weight for pixel } (x,y). \quad W_{D,F}(x,y) = \begin{cases} 1 & \text{if } (x,y) \in F \\ 0 & \text{otherwise} \end{cases}$$

We will compare $D(F,t)$ to threshold T_F with the help of optical flow field to identify if the test car is approaching the leading car or the lane mark. If $D(F,t) < T_F$, the vehicle is safe. Otherwise, there is a potential of danger.

Determining Optical Flow Field

When the relative position of a real object to a camera varies, its image moves on the projection plane of that camera too. The optical flow is the object image movement on the projection plane in sequential image frame (13) (14). It has two components corresponding to the two coordinates in the 2-D image frame. Horn et al. (15) developed an iterative algorithm to determine the optical flow. They derived one constraint equation that the image brightness satisfies. Then, they minimized the sum of the errors in the objective function for the rate of change of image brightness to get the optical flow. Enkelmann et al. (16) expanded the one constraint equation to three. Solving the equations would give the optical flow directly. We employed Enkelmann et al.'s equations to calculate the optical flow.

The brightness satisfies the following differential equation:

$$\frac{dB}{dt} = 0 \quad (3)$$

That is,

$$\frac{\partial B}{\partial x} \frac{\partial x}{\partial t} + \frac{\partial B}{\partial y} \frac{\partial y}{\partial t} + \frac{\partial B}{\partial t} = 0 \quad (4)$$

Take the partial derivative of the above equation with respect to x and y , we have

$$\frac{\partial^2 B}{\partial x^2} \frac{\partial x}{\partial t} + \frac{\partial^2 B}{\partial x \partial y} \frac{\partial y}{\partial t} + \frac{\partial^2 B}{\partial x \partial t} = 0 \quad (5)$$

$$\frac{\partial^2 B}{\partial x \partial y} \frac{\partial x}{\partial t} + \frac{\partial^2 B}{\partial y^2} \frac{\partial y}{\partial t} + \frac{\partial^2 B}{\partial y \partial t} = 0 \quad (6)$$

Then we have three equations (4, 5 and 6) and two unknowns ($\frac{\partial x}{\partial t}$ and $\frac{\partial y}{\partial t}$).

Rewrite the equation as:

$$\mathbf{A}\mathbf{u} = \mathbf{b} \quad (7)$$

where,

$$\mathbf{A} = \begin{pmatrix} B_x & B_y \\ B_{xx} & B_{xy} \\ B_{xy} & B_{yy} \end{pmatrix}, \quad \mathbf{u} = \begin{pmatrix} x_t \\ y_t \end{pmatrix} \equiv \begin{pmatrix} u \\ v \end{pmatrix}, \quad \mathbf{b} = \begin{pmatrix} -B_t \\ -B_{xt} \\ -B_{yt} \end{pmatrix}$$

Where, the subscript, x, y or t , of B , means the partial derivative of B with respect to x, y or t , e.g. $B_x = \partial B / \partial x$ and $B_{yt} = \partial^2 B / \partial y \partial t$.

Since there are three equations and two unknown variables, in general, we have three lines that form a triangle in the (u, v) plane. The optical flow (u, v) with minimal errors is the center of the inside tangent circle of the triangle as shown in Figure 17.

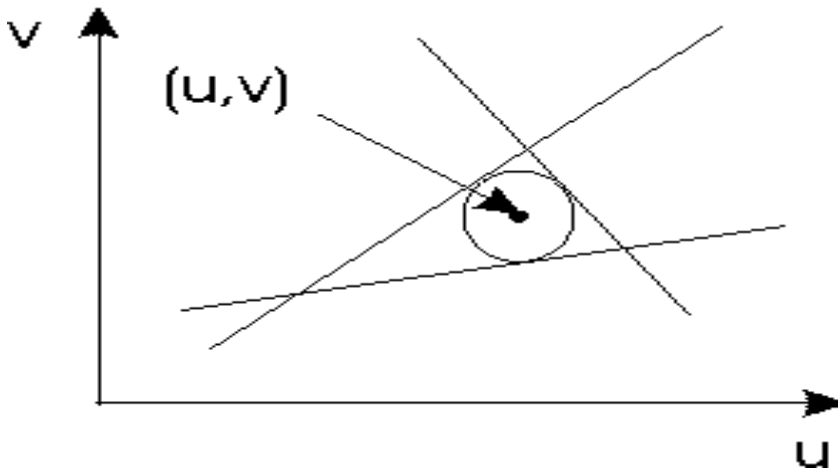


Figure 17. Determining optical flow.

Since the difference image pixels with $D(x,y,t)=1$ are more crucial, we define the aggregate optical flow for difference image in different areas at time t as:

$$U_L(F_L, t) = \sum_{(x,y) \in F_L} W_{u,L}(x,y)u(x,y,t)D(x,y,t) \quad (8)$$

$$U_R(F_R, t) = \sum_{(x,y) \in F_R} W_{u,R}(x,y)u(x,y,t)D(x,y,t) \quad (9)$$

$$V_{TOP}(F_{TOP}, t) = \sum_{(x,y) \in F_{TOP}} W_{v, TOP}(x,y)v(x,y,t)D(x,y,t) \quad (10)$$

$$V_{BOT}(F_{BOT}, t) = \sum_{(x,y) \in F_{BOT}} W_{v, BOT}(x,y)v(x,y,t)D(x,y,t) \quad (11)$$

$$U_{L, BOT}(F_{L, BOT}, t) = \sum_{(x,y) \in F_{L, BOT}} W_{u, L, BOT}(x,y)u(x,y,t)D(x,y,t) \quad (12)$$

$$U_{R, BOT}(F_{R, BOT}, t) = \sum_{(x,y) \in F_{R, BOT}} W_{u, R, BOT}(x,y)u(x,y,t)D(x,y,t) \quad (13)$$

$$V_{L, BOT}(F_{L, BOT}, t) = \sum_{(x,y) \in F_{L, BOT}} W_{v, L, BOT}(x,y)v(x,y,t)D(x,y,t) \quad (14)$$

$$V_{R, BOT}(F_{R, BOT}, t) = \sum_{(x,y) \in F_{R, BOT}} W_{v, R, BOT}(x,y)v(x,y,t)D(x,y,t) \quad (15)$$

Where $W_{..}(x,y)$ is a weight of pixel (x,y) for optical flow component u or v in different areas. If (x,y) is in the corresponding area, $W_{..}(x,y)=1$. Otherwise $W_{..}(x,y)=0$.

VISION GUIDANCE SCHEME

Analysis for Vision Guidance

If $D(F, t) \leq T_F$, the test vehicle is safe. We increase the vehicle speed gradually. If the speeds reach the speed limit, we keep on that speed.

If $D(F, t) > T_F$, the test vehicle is either approaching the leading vehicle or the lane mark.

If $U_L < 0$, $U_R > 0$, $V_{TOP} > 0$ and $V_{BOT} < 0$, the test vehicle is approaching the leading car or an obstacle. We need reduce the speed. See Figure 18.

If $U_{L, BOT} > T_U > 0$, $U_{R, BOT} > T_U > 0$, $V_{L, BOT} < -T_V < 0$ and $V_{R, BOT} < -T_V < 0$, the vehicle is approaching the left side lane mark, such as, the road has right curvature and the vehicle heads straight forward, or the road is straight forward and the vehicle heads left. See Figure 19 (a). We need turn right and reduce the speed.

If $U_{L, BOT} < -T_U < 0$, $U_{R, BOT} < -T_U < 0$, $V_{L, BOT} < -T_V < 0$ and $V_{R, BOT} < -T_V < 0$, the vehicle is approaching the right side lane mark, such as, the road has left curvature and the

vehicle heads straight forward, or the road is straight forward and the vehicle heads right. See Figure 4 (b). We then turn left and reduce the speed.

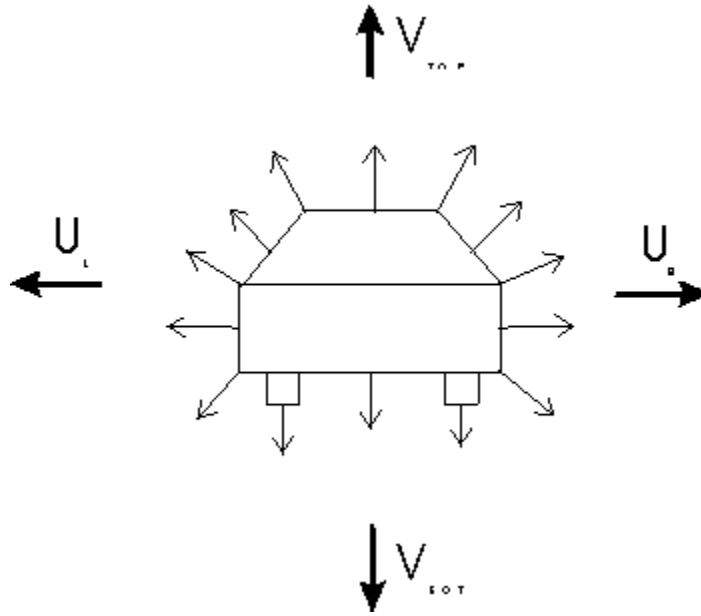


Figure 18. Optical flow field when approaching the leading vehicle.

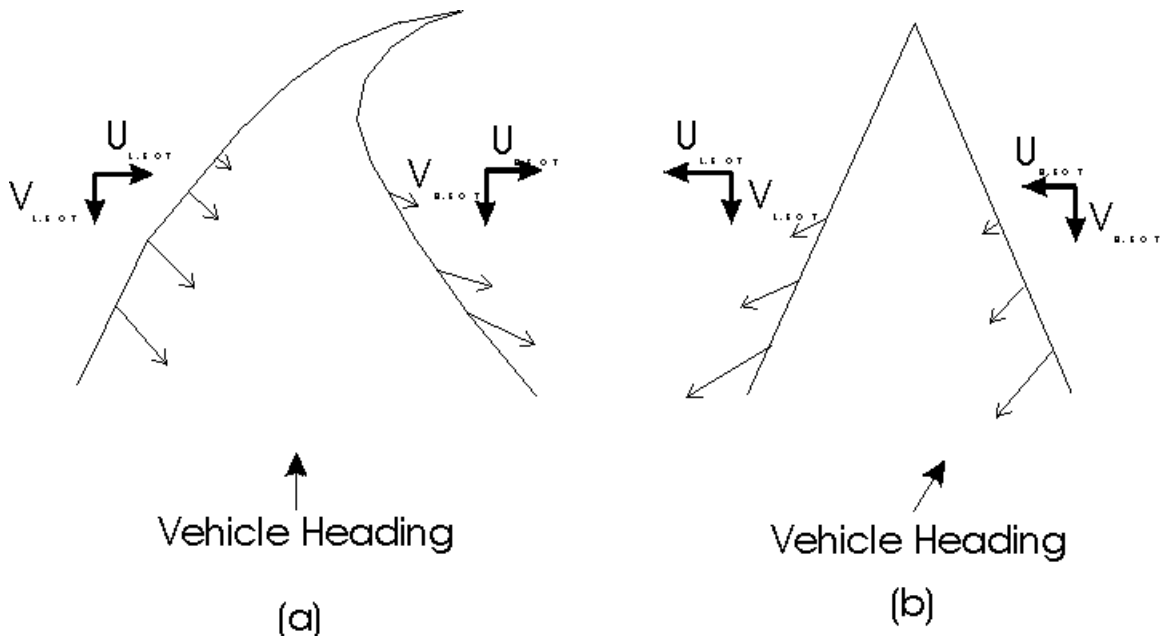


Figure 19. Optical flow field when approaching the lane mark.

- (a) Right road curvature and straight forward vehicle heading direction.
- (b) Straight forward road and right vehicle heading direction.

To pursue the stable performance, we introduced the threshold $T_U > 0$ and $T_V > 0$.

Pseudo Code for Vision Guidance

Following is the pseudo code for the autonomous vehicle vision guidance problem.

```

calculate  $D(x,y,t)$  and  $D(F,t)$ 
if ( $D(F,t) \leq T_F$ )
{ increase vehicle speed gradually until it reaches speed limit }
else
{ calculate  $u(x,y,t)$  and  $v(x,y,t) \forall D(x,y,t) = 1$ 
  calculate  $U_L, U_R, V_{TOP}, V_{BOT}, U_{L,BOT}, U_{R,BOT}, V_{L,BOT}, V_{R,BOT}$ 
  if ( $U_L < 0, U_R > 0, V_{TOP} > 0, V_{BOT} < 0$ )
  { reduce the vehicle speed }
  if ( $U_{L,BOT} > T_U, U_{R,BOT} > T_U, V_{L,BOT} < -T_V, V_{R,BOT} < -T_V$ )
  { turn right and reduce speed }
  elseif ( $U_{L,BOT} < -T_U, U_{R,BOT} < -T_U, V_{L,BOT} < -T_V, V_{R,BOT} < -T_V$ )
  { turn left and reduce speed }
  else
  { set turn angle to zero }
}
if the vehicle speed exceeds the speed limit, set it to the speed limit
if the vehicle turning angular rate exceeds the limit, set it to the limit

```

RESULTS, DISCUSSION AND FUTURE WORK

We built a simulator with OpenGL, a widely used computer graphic language, to test the vision guidance scheme. See Figure 20 for the look of the simulator. The simulator consists of the road, field, roadside trees, sky and a leading vehicle.

We set the speed of the leading vehicle to 10 mph (16 km/h). The speed limit of the test vehicle is 20 mph (32 km/h). The turning angular rate limit of the test vehicle is 30 degrees per second.

Employing these vision guidance schemes mentioned above, the test vehicle will accelerate from static to its speed limit. If approaching the leading vehicle, it would reduce the speed to around 10 mph (16 km/h), the speed of leading vehicle. That is, the scheme can avoid the rear-end collision.

When approaching the road curvature, the test vehicle steers itself according to the curve direction and reduce the speed to around 6 mph (10.6 km/h). The test vehicle makes two turns following the road curvature, then it proceeded to the side of the road. This resulted due to the errors in the calculation of optical flow field. Since the optical flow field is erratic, that would influence the aggregated

optical flow parameter. Due to erratic optical flow field the vehicle might miss some proper action when approaching the side of the lane. The scheme can still perform

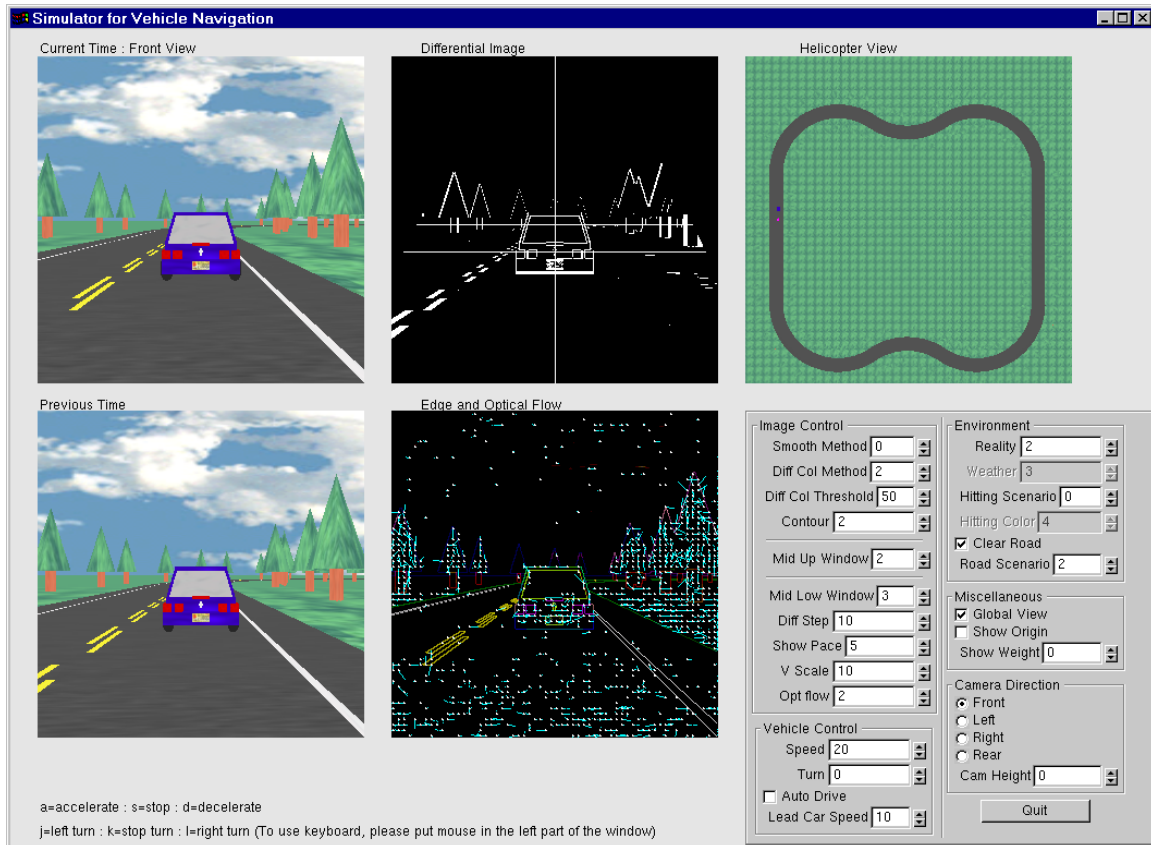


Figure 20. The Simulator.

- Upper left window is the current time image
- Lower left window is the previous time image
- Upper mid window is the difference image
- Lower mid window is the edge and optical flow field
- Upper right window is the helicopter view/global view
- Lower right part is the user interface

well even when the optical flow field is erratic. It indicates that our vision guidance scheme is reasonable. We need a more sophisticated method for calculating the optical flow to let the scheme be more reliable.

If there was an object tree in front of the vehicle, the vehicle would reverse (with negative speed) and go forward (with small positive speed) and reverse again to form a loop. The reason for this occurrence is following: our scheme would reduce the speed even to negative if there was an obstacle. However, if the test

vehicle had negative speed, we would not have the condition ($U_L < 0$, $U_R > 0$, $V_{TOP} > 0$ and $V_{BOT} < 0$), simultaneously. The scheme would determine that it is safe to accelerate, and the vehicle would go forward. Since there was an obstacle, it would reduce the speed again. Similarly, the proposed scheme can avoid the static obstacle too.

Currently, all the weights are set to 1 in the the scheme. The scheme may have a different distribution to produce a better vision guidance performance. All the thresholds are pre-determined in this paper. A sophisticated and reliable scheme, should be self-adaptive in the future. As mentioned above, the optical flow field needs to be more accurate. Practical operation requires, the speed limit of the test vehicle should be increased to the actual speed limit on the road. The scheme needs to be tested under the different scenarios when there are more surrounding vehicles operating in different road conditions. The lane changing mechanism should be incorporated in the vision guidance scheme for a more comfortable driving experience.

CONCLUSIONS

The vehicle vision guidance scheme proposed in this paper is reasonable. It always avoid collisions with both the leading vehicle and static objects. It can follow the lane mark. Only the differential image and optical flow on the pixel with ($D(x,y,t) = 1$) are calculated. It keeps the calculation effort to a minimum. Therefore, the scheme is suitable for real-time application.

For better vision guidance performance, the accuracy of optical flow needs to be enhanced. For easier driving, the lane switching schemes need to be studied.

REFERENCES

1. Masaki, I. (editor)(1992) *Vision-based Vehicle Guidance*, Springer-Verlag.
2. Ulmer, B. (1994) VITA II - Active Collision Avoidance in Real Traffic. *Proceedings of the Intelligent Vehicle '94 Symposium*, Paris, France, pp. 1-6.
3. Schiffmann, J.K. and Widmann, G.R. (1997) Model-based Scene Tracking Using Radar Sensors for Intelligent Automotive Vehicle Systems. *Proceedings of the 1997 IEEE Conference on Intelligent Transportation Systems ITSC* Boston, Massachusetts, pp. 421-426.
4. Kornhauser, A.L. (1991) Neural Network Approaches for Lateral Control of Autonomous Highway Vehicles. *Vehicle Navigation and Information Systems Conference Proceedings (Part 2 of 2)*. Society of Automotive Engineers Technical Paper Series 912871 pp. 1143-1151.
5. Mammar, S. (1997) Lateral Vehicle Control Using Gain Scheduled H_{∞} Controllers. *Proceedings of the 1997 IEEE Conference on Intelligent Transportation Systems ITSC* Boston, Massachusetts, pp. 248-253.
6. Hatipoglu, C.; Ozbay, H.; Ozguner, U. and Sahin, T.B. (1997) H_{∞} Controller Design for Automatic Steering of Vehicles with Modeled Time Delays. *Proceedings of the 1997 IEEE Conference on Intelligent Transportation Systems ITSC*, Boston, Massachusetts, pp. 260-265.
7. Stiller, C.; Poechmueller, W. and Huertgen, B. (1997) Stereo Vision in Driver Assistance Systems. *Proceedings of the 1997 IEEE Conference on Intelligent Transportation Systems ITSC*. Boston, Massachusetts, pp. 888-893.
8. Meier, E.B. and Ade, F. (1997) Tracking Cars in Range Image Sequences. *Proceedings of the 1997 IEEE Conference on Intelligent Transportation Systems ITSC*. Boston, Massachusetts, pp. 105-110.
9. Betke, M.; Haritaoglu E. and Davis L.S. (1997) Highway Scene Analysis in Hard Real-Time. *Proceedings of the 1997 IEEE Conference on Intelligent Transportation Systems ITSC*. Boston, Massachusetts, pp. 812-817.
10. Weng, J.J. and Huang, T.S. (1993) 3-D Motion Analysis from Image Sequences Using Point Correspondences. *Handbook of Pattern Recognition and Computer Vision*, edited by Chen, C.H.; Pau, L.F. and Wang, P.S.P., World Scientific Publishing Co., pp. 395-441.

11. Giachetti, A.; Campani, M.; Sanni, R. and Succi, A. (1994) The Recovery of Optical Flow for Intelligent Cruise Control. *Proceedings of the Intelligent Vehicle '94 Symposium*, Paris, France, pp. 91-96.
12. Sonka, M.; Hlavac, V. and Boyle, R. (1998) *Image Processing, Analysis, and Machine Vision (2nd Ed.)* PWS Publishing.
13. Koenderink, J.J. (1985) Space, Form and Optical Deformations. *Brain Mechanisms and Spatial Vision*, edited by Ingle, D.J., Jeannerod, M. and Lee, D.N., Martinus Nijhoff Publishers. pp. 31-58.
14. Davies, E.R. (1997) *Machine Vision: Theory, Algorithms, Practicalities (2nd Ed.)*, Academic Press.
15. Horn, B.K.P. and Schunck, B.G. (1981) Determining Optical Flow. *Artificial Intelligence*, Vol. 17, pp. 185-203.
16. Enkelmann, W.; Gengenbach, V.; Kruger, W.; Rossle, S. and Tolle, W. (1994) Obstacle Detection by Real-Time Optical Flow Evaluation. *Proceedings of the Intelligent Vehicle '94 Symposium*, Paris, France, pp. 97-102.